ESC HEART FAILURE
ESC Heart Failure 2020; **7**: 4040–4050
Published online 24 September 2020 in Wiley Online Library (wileyonlinelibrary.com) **DOI:** 10.1002/ehf2.13013

ORIGINAL RESEARCH ARTICLE

Reverse electromechanical modelling of diastolic dysfunction in spontaneous hypertensive rat after sacubitril/valsartan therapy

Yen-Ling Sung PhD[1,2†], Ting-Tse Lin MD, PhD[1,3,4†], Jhen-Yang Syu MS[1], Hung-Jui Hsu MS[1], Kai-Yuan Lin MS[1], Yen-Bin Liu MD, PhD[4,5*] and Shien-Fong Lin PhD[1*]

[1]*Institute of Biomedical Engineering, College of Electrical and Computer Engineering, National Chiao Tung University, Hsinchu, 300, Taiwan;* [2]*Department of Electrical and Computer Engineering, National Chiao Tung University, Hsinchu, Taiwan;* [3]*Department of Internal Medicine, National Taiwan University Hospital Hsin-Chu Biomedical Park Branch, Hsinchu, Taiwan;* [4]*Department of Internal Medicine, National Taiwan University College of Medicine, Taipei, Taiwan;* [5]*Department of Internal Medicine, National Taiwan University Hospital, Taipei, Taiwan*

Abstract

Aims Hypertension is a significant risk for the development of left ventricular hypertrophy, diastolic dysfunction, followed by heart failure and sudden cardiac death. While therapy with sacubitril/valsartan (SV) reduces the risk of sudden cardiac death in patients with heart failure and systolic dysfunction, the effect on those with diastolic dysfunction remains unclear. We hypothesized that, in the animal model of hypertensive heart disease, treatment with SV reduces the susceptibility to ventricular arrhythmia.

Methods and results Young adult female spontaneous hypertensive rats (SHRs) were randomly separated into three groups, which were SHRs, SHRs treated with valsartan, and SHRs treated with SV. In addition, the age-matched and weight-matched Wistar Kyoto rats were considered as controls, and there were 12 rats in each group. *In vivo* ventricular tachyarrhythmia induction and *in vitro* optical mapping were used to measure the inducibility of ventricular arrhythmias and to characterize the dynamic properties of electrical propagation. The level of small-conductance Ca^{2+}-activated potassium channel type 2 (KCNN2) was analysed in cardiac tissue. Compared with SHR with left ventricular hypertrophy, treatment with SV significantly improved cardiac geometry (relative wall thickness, 0.68 ± 0.11 vs. 0.76 ± 0.13, $P < 0.05$) and diastolic dysfunction (isovolumetric relaxation time, 59.4 ± 3.2 vs. 70.5 ± 4.2 ms, $P < 0.05$; deceleration time of mitral E wave, 46 ± 4.8 vs. 42 ± 3.8, $P < 0.05$). The incidence of induced ventricular arrhythmia was significantly reduced in SHR treated with SV compared with SHR (ventricular tachycardia, 1.14 ± 0.32 vs. 2.91 ± 0.5 episodes per 10 stimuli, $P < 0.001$; ventricular fibrillation, 1.72 ± 0.31 vs. 5.81 ± 0.42 episodes per 10 stimuli, $P < 0.001$). The prolonged action potential duration (APD) and increase of the maximum slope of APD restitution were observed in SHR, while the treatment of SV improved the arrhythmogeneity (APD, 37.12 ± 6.18 vs. 92.41 ± 10.71 ms at 250 ms pacing cycle length, $P < 0.001$; max slope 0.29 ± 0.01 vs. 1.48 ± 0.04, $P < 0.001$). These effects were strongly associated with down-regulation of KCNN2 (0.38 ± 0.07 vs. 0.74 ± 0.12 ng/ml, $P < 0.001$). The treatment of SV also decreased the level of N-terminal pro-B-type natriuretic peptide, cardiac bridging integrator-1, and intramyocardial fibrosis of SHR.

Conclusions In conclusion, synergistic blockade of the neprilysin and the renin–angiotensin system by SV in SHRs results in KCNN2-associated electrical remodelling in ventricle, which stabilizes electrical dynamics and attenuates arrhythmogenesis.

Keywords Hypertensive heart disease; Diastolic dysfunction; Sacubitril/valsartan; Ventricular arrhythmogenesis; Small-conductance Ca^{2+}-activated potassium channel type 2; Cardiac bridging integrator-1

Received: 6 March 2020; Revised: 2 September 2020; Accepted: 2 September 2020
**Correspondence to: Shien-Fong Lin, Institute of Biomedical Engineering, College of Electrical and Computer Engineering, National Chiao Tung University, 1001 Ta-Hsueh Road, Hsinchu 300, Taiwan. Email: linsf5402@nctu.edu.tw*
Yen-Bin Liu, Department of Internal Medicine, National Taiwan University College of Medicine, Taipei, Taiwan. Email: yenbin@ntu.edu.tw
† Yen-Ling Sung and Ting-Tse Lin contributed equally to this work.

Introduction

The diagnostic and therapeutic assessments of cardiac diseases in the last decades have been focusing on heart failure (HF) with reduced ejection fraction (HFrEF), which was considered as the most common HF.[1,2] However, diastolic dysfunction, a hallmark of hypertensive heart disease and left ventricular hypertrophy (LVH), followed by HF with preserved ejection fraction, has been steadily increasing prevalence for approximately more than 50% of all HF,[3,4] with the rate of hospitalization that continues to rise globally. Furthermore, HFrEF has numerous pharmacological and device-based treatment options available, but no treatments have proven to be beneficial in reducing hospitalization and mortality rates in patients with diastolic dysfunction.[2,5]

Recently, a new strategy using sacubitril/valsartan (SV) was suggested as a therapeutic option to target HF pathophysiology, combining the neprilysin (NEP) inhibitor (sacubitril) and renin–angiotensin system (RAS) inhibitor (valsartan).[6] SV is a first-in-class medicine that has been proven to minimize the risk of non-sustained and sustained ventricular tachycardia in HFrEF patients.[7,8] Previous studies have shown that LCZ696 improves systolic function, electrophysiological benefits, and down-regulation of sodium and potassium channel protein expression, which are important contributors to systolic dysfunction-related ventricular arrhythmia.[9,10] On the other hand, the rate of sudden cardiac death (SCD) is 0.3 per 100 patient-years in hypertensive patients without cardiovascular diease.[11] SCD even accounts for around 20% of deaths in hypertensive patients with diastolic dysfunction and HF, which is also associated with malignant ventricular arrhythmia.[2,12–15] The hypertensive cardiac remodelling, composing of LVH, diastolic dysfunction, and neurohormonal changes, is known as the risk of SCD. The changes of N-terminal pro-B-type natriuretic peptide (NT-proBNP) and cardiac bridging integrator-1 (cBIN-1), which were related to mechanical stress of ventricle and the stability of cardiac T-tubule membrane, respectively, were considered as the surrogate markers of cardiovascular outcomes in HF patients.[3,16] The use of RAS inhibitors improves the cardiovascular outcomes in hypertensive patients.[17] However, there is paucity of data on the clinical benefits of SV on ventricular arrhythmia and the electromechanical features. Here, we implemented a rodent model of spontaneous hypertensive rat (SHR) with diastolic dysfunction and ventricular hypertrophy to investigate the therapeutic effects of SV and the underlying mechanisms of susceptibility to ventricular arrhythmia.

Materials and methods

Animals

The animal study protocol was approved by the Animal Care and Use Committee of National Chiao Tung University. Animal experiments were performed conforming to the National Institutes of Health guidelines (Guide for the Care and Use of Laboratory Animals). At 18 weeks of age, female SHRs were randomly assigned to three groups (N = 12 each): SHRs with normal saline (SHR), SHRs with valsartan (160 mg/1 kg; SHR-VL), and SHRs with SV (300 mg/1 kg; SHR-SV, matching clinical dosage of 98/102 mg). An additional group of female Wistar Kyoto (WKY) rats (N = 12) served as the control group with normal saline. The randomized groups were assessed for equal median and range of body mass (221.8 ± 5.1 g). Rats were provided with drugs and the same volume of saline by oral gavage every day for 2 weeks.

Echocardiography

Transthoracic echocardiography was performed by a technician blinded to the treatment. Rats were anaesthetized with isoflurane and placed supine on an electrical heating pad at 37°C under mild anaesthesia maintenance with 1.5% isoflurane/98.5% oxygen. Parasternal long-axis and short-axis two-chamber M-mode views were obtained at the mid-papillary level and averaged to determine left ventricular dimensions at end-systole and end-diastole. Two-dimensional B-mode, M-mode, and pulsed-wave Doppler images were obtained using the high-frequency ultrasound scanner Vevo 2100 Micro-Ultrasound (VisualSonics, Toronto, Canada) equipped with an ultra-high-frequency MS250 linear array transducer (13–24 MHz). Left ventricular end-diastolic dimension, left ventricular end-systolic dimension, the thickness of the interventricular septum (IVSd), and left ventricular posterior wall (PWd) were measured as recommended by the guideline. Calculating the relative wall thickness (RWT) was based on the formula [(PWd + IVSd)/LVIDd, where d is diastolic]. Mitral flow velocity patterns were obtained in the apical four-chamber view with colour Doppler mode. Mitral flow velocity patterns were analysed to determine peak early diastolic filling velocity (E velocity) and peak late diastolic filling velocity during atrial contraction (A velocity), as well as their ratio (E/A ratio), isovolumetric relaxation time (IVRT), and deceleration time of the E wave (DT_E). Because of the high heart rates, which sometimes caused fusion of the E and A waves, we excluded those data from analysis. We indicated the number of rats in each group whose E and A waves could be assessed (WKY, n = 10; SHR, n = 7; SHR-VL, n = 7; and SHR-SV, n = 9).

Non-invasive blood pressure system

The non-invasive blood pressure system was used for all tail-cuff measurements, and the blood pressure

DOI: 10.1002/ehf2.13013

measurement experiments were based on volume changes in the tail. For all, rat was encouraged to walk into the restraint tubes, and the occlusion cuff was placed at the base of the tail. The sensor cuff was placed adjacent to the occlusion cuff. Heating pads were preheated from 33°C to 35°C. The measurement was conducted in a designated quiet area, where rat was acclimatized for a 1 h period before experiments began. The rat was warmed for 5 min before and during blood pressure recordings. To measure blood pressure, the occlusion cuff is pressurized to at least 250 mmHg and deflated over 15 s. The sensor cuff detects changes in the tail volume as the blood returns to the tail during the occlusion cuff deflation. Each recording session consisted of 15 to 25 inflation and deflation cycles per set, of which the first 5 cycles were not used in the analysis. Rat was habituated for at least five consecutive days before baseline blood pressure measurements.

In vivo induction of ventricular arrhythmias

Programmed electric stimulation was applied to induce ventricular arrhythmia. In brief, rats were anaesthetized by an injection of 30 mg/kg of zoletil, and a tracheotomy was performed to assist breathing after the thoracotomy. An S1–S2 pacing protocol was used with eight S1 stimuli (cycle length 70 ms) followed by an S2 premature stimulation. The S1–S2 coupling interval started from 65 ms and then sequentially decreased by 5 till 20 ms. The numbers of ventricular arrhythmias are calculated by the successes of induced ventricular arrhythmias within 10 stimuli per rat. The duration is defined as the time of ventricular arrhythmias in each number of induced episodes. The induced ventricular arrhythmias were classified by the observer according to the guidelines known as The Lambeth Conventions,[18] which defined VT as a run of four or more consecutive ventricular premature beats and VF as a signal with indistinguishable QRS deflections whose rate changes from beat to beat.

Optical mapping

The hearts were isolated for optical mapping study. The rats were anaesthetized with 1.5% isoflurane/98.5% oxygen inhalation, and the hearts were rapidly excised after the open-chest operation. The coronary artery was perfused with Tyrode's buffer equilibrated with 95% O_2 and 5% CO_2 to maintain a pH of 7.4. Tyrode's solution was included 125 NaCl, 4.5 KCl, 24 $NaHCO_3$, 1.8 NaH_2PO_4, 0.5 $MgCl_2$, 5.5 glucose, 1.8 $CaCl_2$, and 0.1 albumin (in mM). After voltage-sensitive dye, Di-4-ANEPPS (Thermo Fisher Scientific, Massachusetts, USA) was added to perfuse for 10 min, and blebbistatin (20 μM, Tocris Bioscience, Minneapolis, USA) was also perfused to inhibit contractility of the heart. A CMOS camera (SciMedia, Costa Mesa, CA) was used to collect the induced fluorescence through a 600 nm long-pass filter. Furthermore, the images were loaded to custom-design software for image optimization and calculation.

The conduction velocity (CV) map was calculated using the isochronal map, which was constructed based on the optical mapping data to show the cardiac electrical propagation. The boundaries between successive activation times in the isochronal map were identified and fitted with polynomial curves. Normal vectors of the polynomial curve were calculated to represent the direction of electrical propagation. Moreover, the standard deviation of the conduction angles was calculated and designated as STD_{angle}. A large STD_{angle} indicates that electrical propagation is more heterogeneous.

Enzyme-linked immunosorbent assay for protein quantification

The heart was harvested after optical mapping, and the left ventricles were homogenized in T-PER reagent (Thermo Fisher Scientific, Massachusetts, USA), containing protease inhibitors (Roche, California, USA) and phosphatase inhibitors (Roche, California, USA). The total protein concentration was determined using a Bradford Assay (Bio-Rad, California, USA). Bridging integrator-1 (Cat. No. MBS2019820, MyBioSource, California, USA) and the level of gene expression KCNN2 encoding small-conductance calcium-activated potassium channel subfamily N, member 2 (Cat. No. MBS160599, MyBioSource, California, USA) were measured by an enzyme-linked immunosorbent assay (Cat. No. MBS160599, MyBioSource, California, USA).

Venous blood samples were collected in BD Vacutainer™ blood collection tubes (BD, New Jersey, USA) containing K2EDTA. After centrifugation (10 000 × *g*) for 20 min at 4°C, the supernatant was collected and stored in −80°C freezer for later enzyme-linked immunosorbent assay analysis. NT-proBNP levels were analysed using a commercial EIA kit (Cat. No. EIA-BNP-1, RayBiotech, Georgia, USA) according to the manufacturer's instructions.

Statistical analysis

Comparisons of data between each pair of four groups were performed by using the Kruskal–Wallis test with Dunn's *post hoc* test when the data were lacking normal distribution or otherwise by the one-way ANOVA with Tukey's *post hoc* tests. A *P*-value <0.05 was considered statistically significant. All data were reported as mean ± standard error. OriginLab (OriginLab, Massachusetts, USA) and GraphPad Prism 7 (GraphPad Software, California, USA) software packages were used in our analysis.

DOI: 10.1002/ehf2.13013

Results

Sacubitril/valsartan reduced blood pressure and ameliorated ventricular hypertrophy

The haemodynamic measurements and echocardiographic analysis revealed that systolic blood pressure, diastolic blood pressure, mean arterial pressure, IVSd, RWT, and IVRT significantly increased in all SHR groups (*Table 1*). However, the administration of SV significantly decreased systolic blood pressure, diastolic blood pressure, and mean arterial pressure than SHR and SHR-VL. RWT and IVRT of SHR-SV significantly decreased to 0.68 ± 0.11 and 59.4 ± 3.2 ms, compared with SHR (RWT, 0.76 ± 0.13; IVRT, 70.5 ± 4.2 ms), respectively. Left ventricular end-diastolic dimension, left ventricular end-systolic dimension, PWd, and left ventricular ejection fraction remained at the same level after 2 week treatment. In the SHR-SV rats, deceleration time of the E wave significantly increased than SHR and SHR-V (WKY: 49 ± 4.1 vs. SHR: 42 ± 3.8 vs. SHR-VL: 43 ± 4.2 vs. SHR-SV: 46 ± 4.8). For all, these results show that the administration of SV significantly decreased blood pressure than SHR and SHR-VL as a consequence of the superior protective effect to blood pressure reduction and improving ventricular hypertrophy.

Sacubitril/valsartan shortened the duration of ventricular arrhythmias

Figure 1 shows representative tracings of inducible ventricular arrhythmias. After SV administration, the induced ventricular arrhythmias were more moderate compared with valsartan, and the heart rates were similar to those of WKY, indicating that SV could have a therapeutic effect to restore cardiac rhythms. Notably, the duration of ventricular arrhythmias was always longer than 1 s in SHR, which was not the case in SHR-SV.

Sacubitril/valsartan reduced susceptibility to ventricular arrhythmias

Figure 2A and *2B* shows an increase in the number of VT and VF episodes in SHR hearts, but no arrhythmias were induced in the WKY group. Notably, the number of episodes of ventricular arrhythmias decreased significantly in SHR-SV, whereas SHR-VL hearts have no significant difference in VT episodes (*Figure 2A* and *2B*) (VT: WKY: 0 ± 0.0 vs. SHR: 2.91 ± 0.5 vs. SHR-VL: 2.32 ± 0.48 vs. SHR-SV: 1.14 ± 0.32; VF: WKY: 0 ± 0.0 vs. SHR: 5.81 ± 0.42 vs. SHR-VL: 4.25 ± 0.44 vs. SHR-SV: 1.72 ± 0.31). Meanwhile, the SHR-SV hearts exhibited significantly shorter time of VT and VF duration than the SHR-SV ones (*Figure 2C* and *2D*). Taken together, our experimental evidence suggested that SV is more effective in lowering the susceptibility to ventricular arrhythmia than valsartan.

In vitro optical mapping

We performed optical mapping and analysed the dynamic properties of cardiac electricity on SHR hearts. *Figure 3* shows the effects of SV on action potential duration (APD) and APD

Table 1 General and echocardiographic parameters

Parameter	WKY (n = 12)	SHR (n = 12)	SHR-DIO (n = 12)	SHR-ENT (n = 12)
HR (1/min)	342 ± 10	354 ± 16	352 ± 21	349 ± 13
SBP	105.6 ± 8	148.8 ± 6*	130.2 ± 11*,†	110.1 ± 7†
DBP	89.1 ± 9	142.4 ± 7*	121.2 ± 10†	122.1 ± 8†
MAP	102.1 ± 7	145.2 ± 8*	124.2 ± 8*,†	109.4 ± 7†,‡
LVEDD (mm)	6.4 ± 0.4	6.6 ± 0.3	6.5 ± 0.2	6.4 ± 0.4
LVESD (mm)	4.3 ± 0.1	4.4 ± 0.5	4.3 ± 0.4	4.2 ± 0.3
IVSd (mm)	1.8 ± 0.2	2.4 ± 0.2*	2.3 ± 0.3*	2.4 ± 0.3*
PWd (mm)	2.0 ± 0.3	2.3 ± 0.2	2.2 ± 0.2	2.2 ± 0.4
RWT	0.61 ± 0.07	0.76 ± 0.13*	0.74 ± 0.11*	0.68 ± 0.11*,†,‡
LVEF (%)	71 ± 8	73 ± 12	70 ± 11	72 ± 8
MV E (m/s)	7.7 ± 0.1	7.4 ± 0.3	7.6 ± 0.2	7.9 ± 0.1
MV A (m/s)	3.0 ± 0.1	3.0 ± 0.2	2.9 ± 0.1	2.9 ± 0.2
MV E/A ratio	2.8 ± 0.2	2.8 ± 0.3	2.7 ± 0.3	2.9 ± 0.3
IVRT (ms)	40.5 ± 4.3	70.5 ± 4.2*	65.9 ± 3.2*,†	59.4 ± 3.2*,†,‡
DT_E	49 ± 4.1	42 ± 3.8*	43 ± 4.2*	46 ± 4.8†

DBP, diastolic blood pressure; DT_E, deceleration time of mitral E wave; HR, heart rate; IVRT, isovolumetric relaxation time; IVSd, interventricular septal thickness during diastole; LVEDD, left ventricular end-diastolic dimension; LVEF, left ventricular ejection fraction; LVESD, left ventricular end-systolic dimension; MAP, mean arterial pressure; MV E and A, maximal velocity of mitral annulus during early and late diastole, respectively; PWd, left ventricular posterior wall thickness during diastole; SBP, systolic blood pressure; SHR, spontaneous hypertensive rat; WKY, Wistar Kyoto rats.
$^{*}P < 0.05$ vs. WKY group.
$^{\dagger}P < 0.05$ vs. SHR group.
$^{\ddagger}P < 0.05$ vs. SHR-DIO group.

Figure 1 Schematic representation of ventricular arrhythmia after *in vivo* induction. (A) Normal heart rhythm. (B) Sustained ventricular arrhythmia. (C, D) Ventricular arrhythmia.

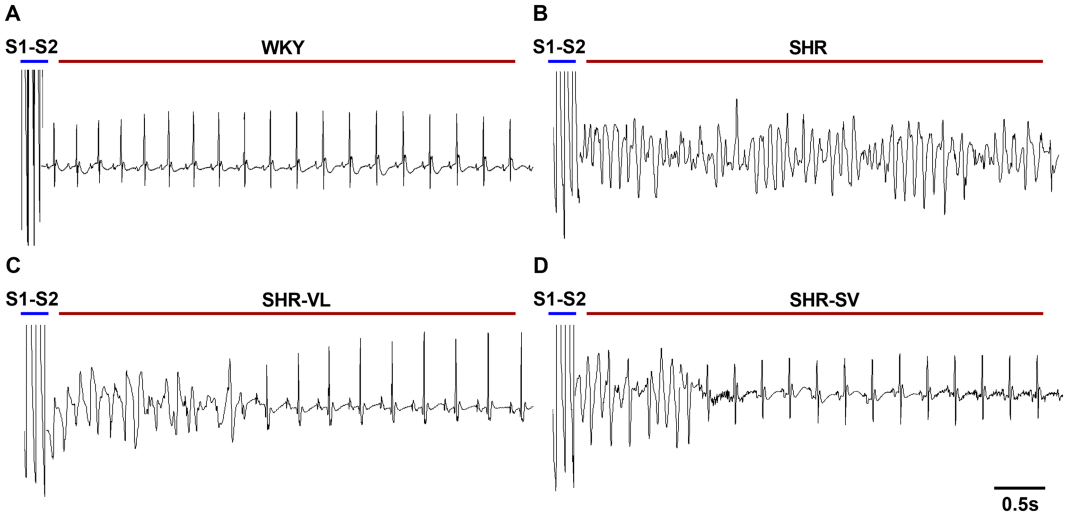

Figure 2 The inducibility of ventricular arrhythmias *in vivo*. (A) Examples of VT and VF response to programmed electrical stimulation. (B) Quantification of induced VT. (C) Quantification of induced VF. (D, E) Quantification of duration of induced VT and VF duration. $^{*}P < 0.05$ and $^{***}P < 0.001$ vs. the WKY group. An unpaired Student's *t*-test was performed for each pair of four groups.

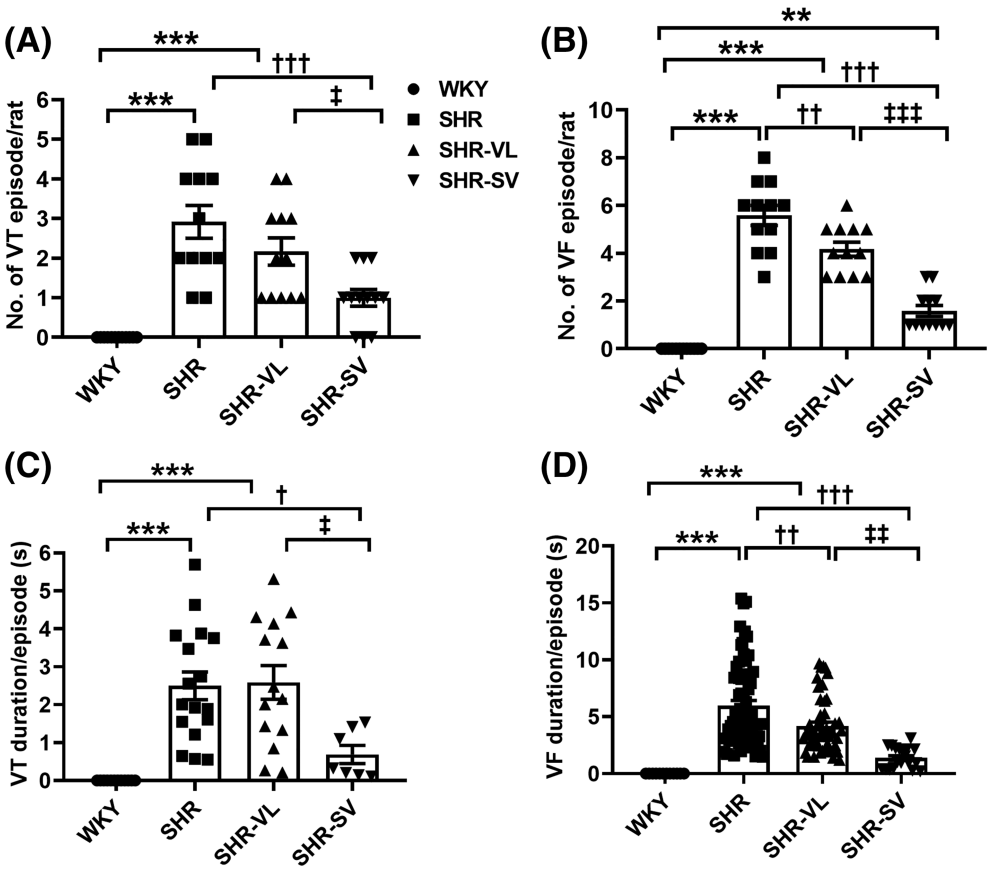

DOI: 10.1002/ehf2.13013

Figure 3 Observation of action potential duration (APD) on the modulation of ion channels. (A) Typical examples of APD at pacing cycle length (PCL) 300 in a normal and hypertensive ventricle. (B) APD at 70% of repolarization at all PCLs. (C) APD_{70} was plotted against diastolic interval, presented as APD restitution curve. (D, E) The slope against all PCLs and higher the maximum slope presented as arrhythmogenicity. $^{***}P < 0.001$ vs. the WKY group. $^{\dagger}P < 0.05$, $^{\dagger\dagger}P < 0.01$, and $^{\dagger\dagger\dagger}P < 0.001$ vs. SHR group. An unpaired Student's *t*-test was performed for each pair of four groups.

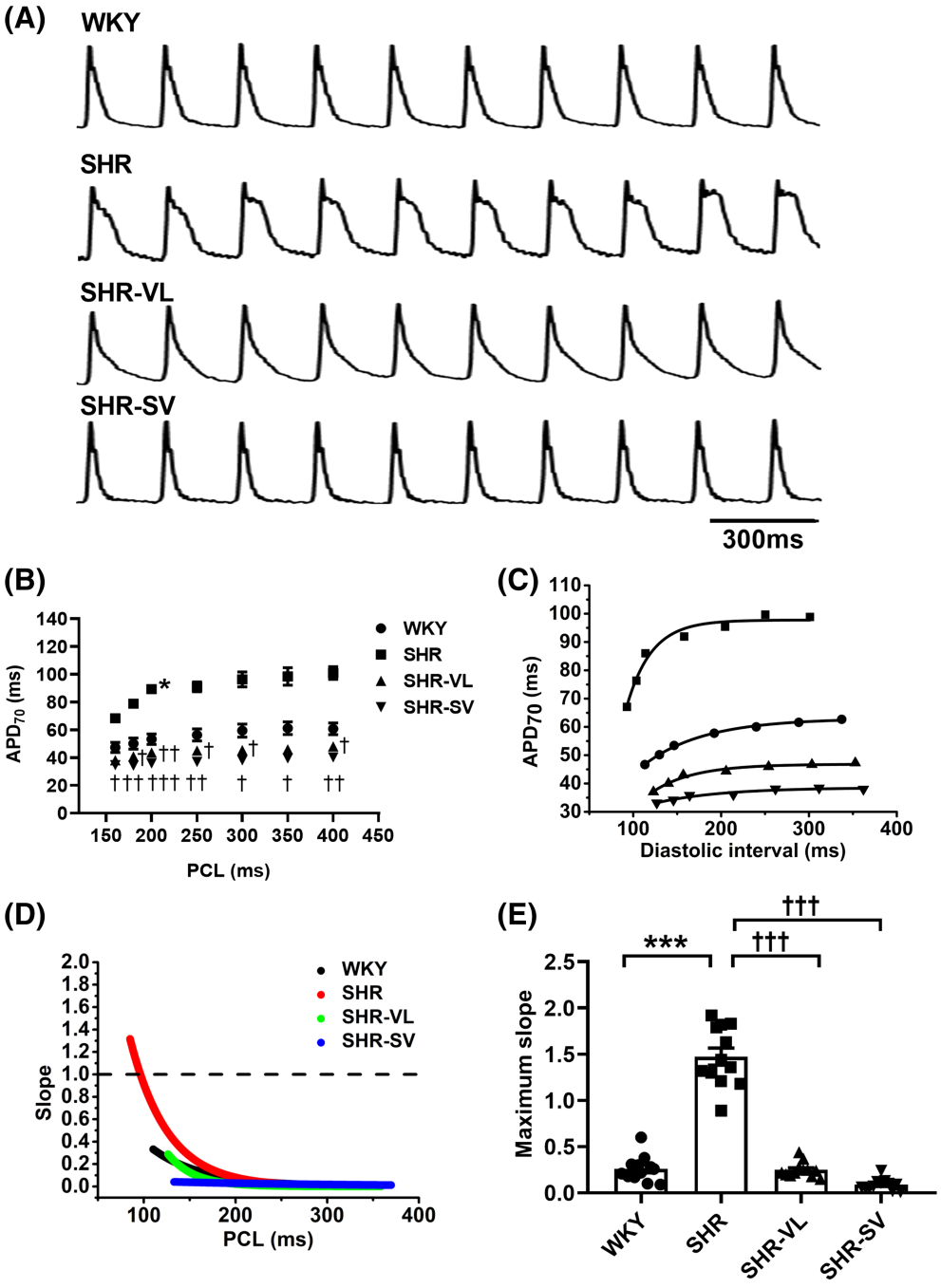

restitution. The ventricles with SV treatment had shorter APD_{70} than SHR, and the long steady state of the plateau was only observed on SHR (*Figure 3A*). APD_{70} was prolonged in SHR, while the deceleration of APD_{70} was observed after valsartan and SV treatment (*Figure 3B*). The slope of APD restitution curves illustrated that treatment groups have the shallower slopes than the SHR group, especially at the shorter pacing cycle lengths (*Figure 3C*). At the diastolic interval of 160 ms, the APD slope in SHR was significantly higher than 1, which implied instability in electrical dynamics and a significantly high risk for arrhythmias (*Figure 3D*). SHR increased the maximum slope of APD restitution ($P < 0.0001$), but it

DOI: 10.1002/ehf2.13013

was similar between WKY and treatment groups (*Figure 3E*). It is noteworthy that treatment with SV ameliorated repolarization heterogeneity and APD alternans.

Figure 4A showed the waveform of the CV map. Smoother electrical propagation and ordered conduction direction was observed in SHR-SV than those of SHR and SHR-VL. However, CVs had no significant difference in all groups (*Figure 4B*). The STD_{angle} was significantly decreased in SHR-SV than SHR and SHR-VL (*Figure 4C*) (WKY: 0.58 ± 0.04 vs. SHR: 0.62 ± 0.06 vs. SHR-VL: 0.52 ± 0.08 vs. SHR-SV: 0.42 ± 0.07). These results demonstrated that the administration of SV effected on normalizing the electrical propagation.

Immunochemical staining

In cardiac structure and intracellular factor responses analysis, the results have shown that interstitial fibrosis is significantly reduced by the administration of SV (*Figure 5A* and *5B*). We found that the mean NT-proBNP in plasma and cBIN-1 levels in the heart are reversal trend (*Figure 5C* and *5D*). Obviously, treatment with SV in SHR could powerfully increase the expression level of cBIN-1 and has significant differences from SHR.

Recent studies have shown that SK2 plays a crucial role in the aetiology of arrhythmias, regarding outward currents that

Figure 4 Sacubitril/valsartan increases the consistency of conduction velocity. (A) The isochronal map is a colour scale of the time taken to activate at each pixel. The time increases in the direction opposite to where the electrodes are placed. Conduction vectors that show the direction of the wave are generated from the activation map. (B) Conduction velocity (CV) at all pacing cycle lengths (PCLs). (C) The standard deviation of the conduction angles (STD_{angle}) of the isochrones map has calculated the difference of standard deviation in the average angle of conduction vectors. $^{\dagger\dagger\dagger}P < 0.001$ vs. SHR group. $^{\ddagger}P < 0.05$ vs. SHR-DIO group. An unpaired Student's *t*-test was performed for each pair of four groups.

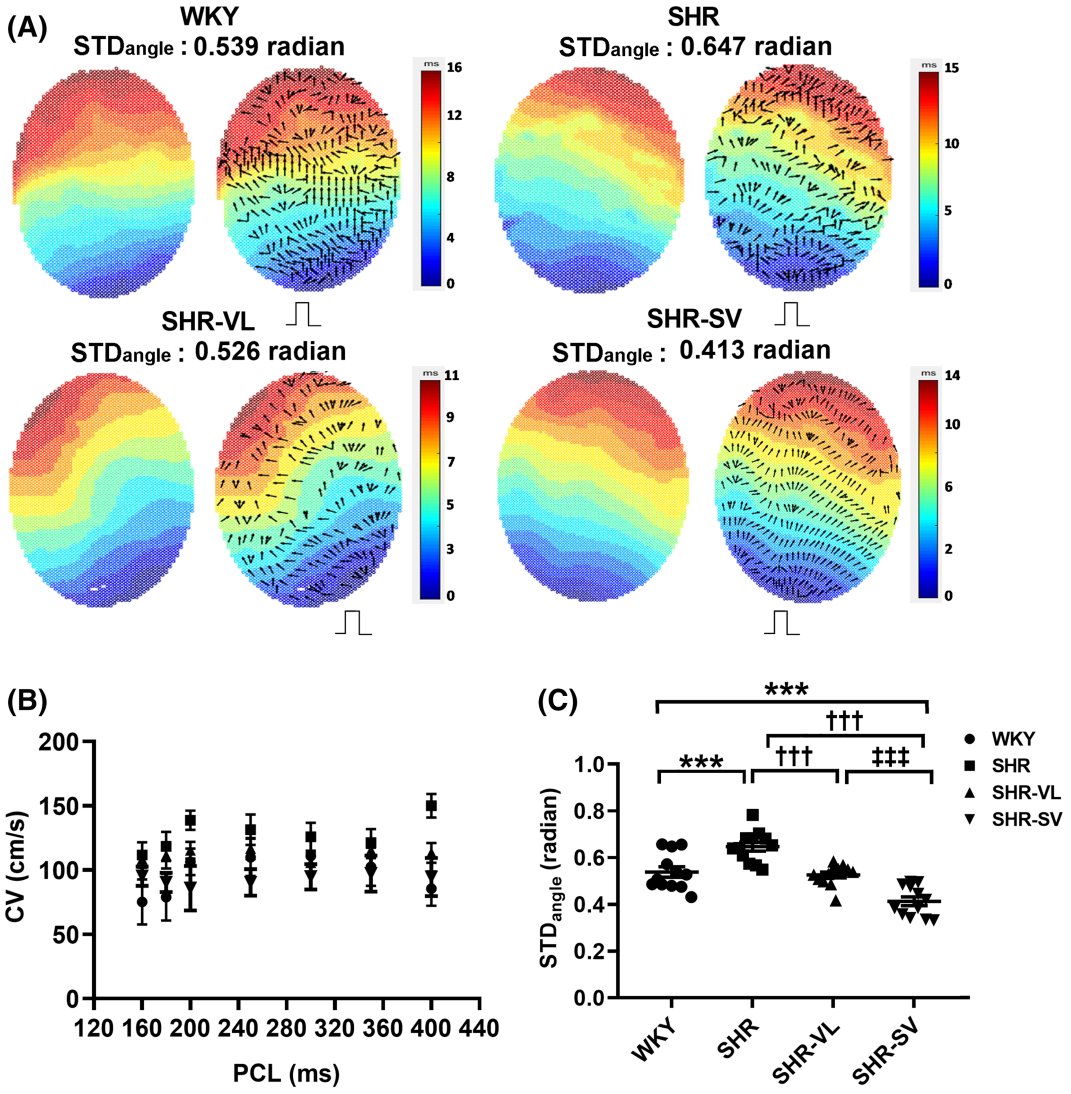

DOI: 10.1002/ehf2.13013

Figure 5 The reversal level of N-terminal pro-B-type natriuretic peptide (NT-proBNP) and bridging integrator-1 (BIN-1) decrease interstitial fibrosis and the cardiac level of KCNN2 protein by sacubitril/valsartan. (A) Examples of Masson's trichrome staining of cross sections of the ventricle. (B) The quantification of fibrosis areas. (C, D) The expression of NT-proBNP and BIN-1 in plasma and heart, respectively. (E) The quantification of the level of KCNN2 protein in ventricular cardiac tissue. $^{*}P < 0.05$, $^{**}P < 0.01$, and $^{***}P < 0.001$ vs. WKY group. $^{\dagger}P < 0.05$, $^{\dagger\dagger}P < 0.01$, and $^{\dagger\dagger\dagger}P < 0.001$ vs. SHR group. An unpaired Student's *t*-test was performed for each pair of four groups.

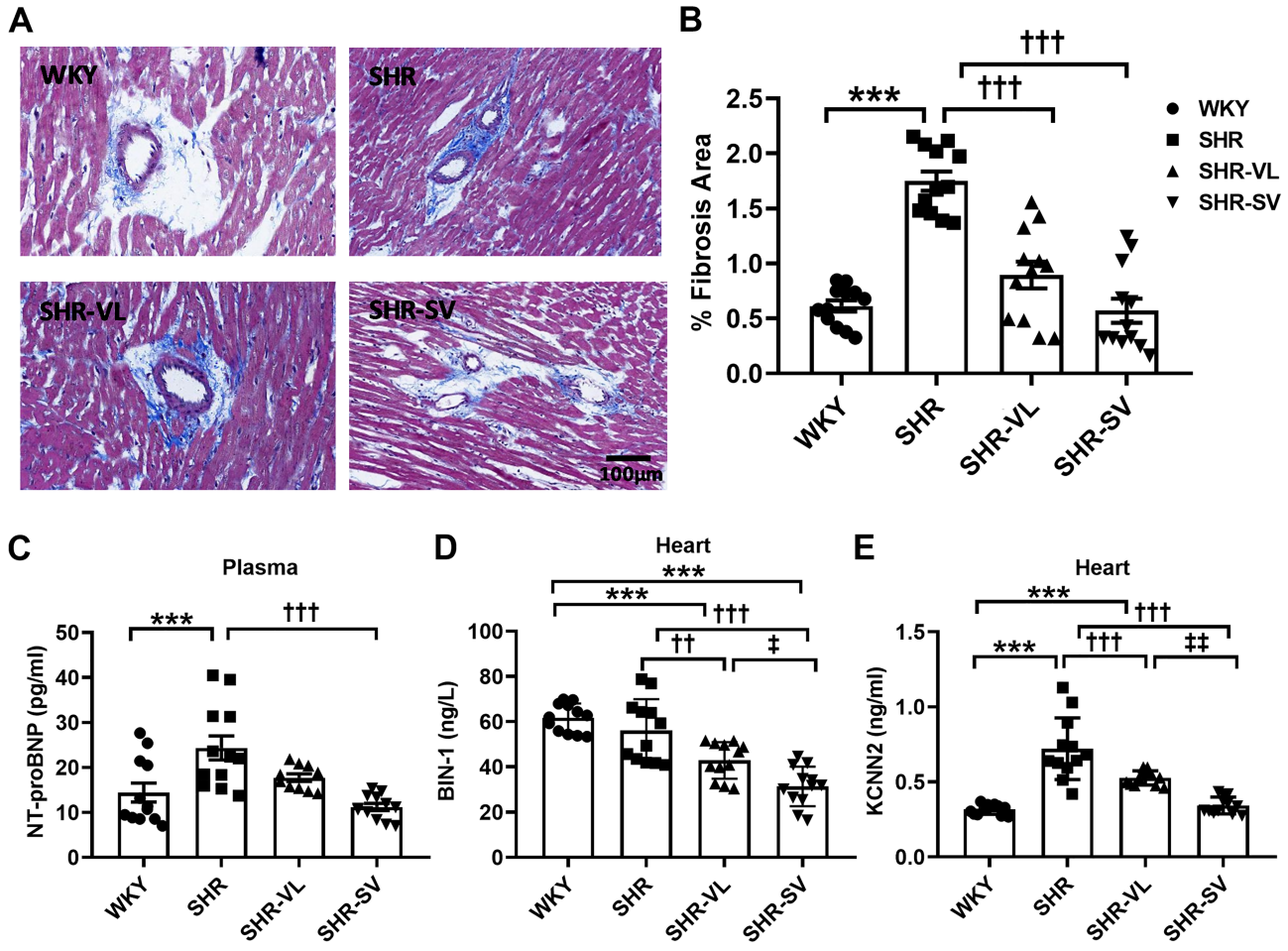

constitute the late repolarization phase of the action potential and Ca^{2+} handling.[19] Further analysis was attempted to elucidate the level of KCNN2, which encodes an integral membrane protein that forms SK2 channels. KCNN2 was overexpressed in SHR than WKY. SV decreases the level of KCNN2 protein significantly than SHR and VL (WKY: 0.34 ± 0.02 vs. SHR: 0.76 ± 0.19 vs. SHR-VL: 0.59 ± 0.02 vs. SHR-SV: 0.39 ± 0.06 ng/ml) (*Figure 5E*).

Discussion

In this study, we investigated the beneficial effects of SV on cardiac electromechanical properties in SHRs with diastolic dysfunction. The main finding is that treatment with SV significantly reduces cardiac hypertrophy and lowers the susceptibility to ventricular arrhythmias than treatment with valsartan and controls. In addition to these apparent clinical outcomes, treatment with SV also modulated repolarization dispersion and alleviated conduction heterogeneity. These beneficial effects on electromechanical properties were highly associated with down-regulation of cardiac KCNN2 protein, whose expression was significantly increased in SHR with diastolic dysfunction.[20]

Patients with systolic HF and intracardiac defibrillator experienced less intracardiac defibrillator therapy, ventricular arrhythmia burden, and even atrial fibrillation in the duration of SV treatment than those of enalapril treatment.[8] These clinical evidence supported the notion that SV is an anti-arrhythmia drug. On the other hand, hypertensive patients also have the risk of SCD, and the associated hypertensive heart disease, including LVH, diastolic dysfunction, and left atrial enlargement, increases the risk of ventricular

DOI: 10.1002/ehf2.13013

arrhythmia.[11] Therefore, our results matched a specific pathophysiology of SCD with the available therapies to improve outcomes in patients with hypertensive heart disease.

The current SHR model, characterized by ventricular hypertrophy and diastolic dysfunction, is associated with increased fibrosis, collagen deposition, and risk of SCD. Areas of fibrosis alter regional conduction patterns and serve as islands of reentry, which is the most common underlying mechanism of sustained ventricular arrhythmia.[21] Therapy with valsartan and SV could be effective to reverse cardiac hypertrophy by blocking RAS.[22] However, as compared with valsartan, treatment with SV could further reverse hypertrophy and reduce cardiac interstitial fibrosis. Neprilysin inhibition increases the circulating levels of natriuretic peptides, which have several cardioprotective effects that counteract the detrimental effects of RAS and sympathetic nervous system activation.[23] The protective effects include vasodilation, natriuresis, and inhibition of the RAS and sympathetic system, and, most important, reduce cardiac inflammation, cell death, hypertrophy, and fibrosis, with the more potential to reverse or reduce left ventricular remodelling than valsartan only.[23] Our results demonstrated less fibrosis of SHR myocytes when treated with SV as compared with valsartan. Furthermore, the reverse of myocardium hypertrophy resulted in reduced arrhythmia inducibility of SHR. On the other hand, as compared with valsartan, SV seems to reduce the risk of HF hospitalization more in women than in men with diastolic HF.[24] The apparent sex difference of the beneficial effect of SV has several mechanisms, and our study (all female WKY and SHR) provides a potential explanation. Our findings raise a hypothesis that the specific phenotype, female hypertensive patients with diastolic dysfunction, may have good response to SV.

We observed very steep APD restitution curve in SHR group, and the treatment with valsartan and SV flattened the curve, which indicated that the ventricle of SHR-SV was electrically more stable and less susceptible to induction of VT/VF.[25] In addition to remodelling of ventricular hypertrophy, ion channels play an essential role in modulating the cardiac action potential for electrical conduction throughout the hypertrophic heart.[26] In respect of systolic HF rat model, Chang *et al*.[9] observed that LCZ696 could up-regulate expression of K^+ channel proteins, including KCNH2, KCNE1, and KCNE 2, which caused shortened APD and ameliorated ventricle arrhythmogeneity of myocardial infarction-related HF. In contrast, in the SHR group, we observed up-regulation of tissue expression of small-conductance Ca^{2+}-activated K^+ (SK and $K_{Ca}2$). The up-regulation was consistent in the valsartan group, but significant down-regulation of SK channel was observed in the SV group, indicating that this electrophysiological feature came from the sacubitril effect. SK channels are unique in that they are gated solely by changes in intracellular Ca^{2+} and hence function to integrate intracellular Ca^{2+} and membrane potentials on a beat-to-beat basis.[27] While increased APD alternans and expression of SK2 channel were observed in the SHR group, the treatment with SV, rather than valsartan, reduced the expression of SK2, which leads to the flattened maximal slope and the ventricle homogeneity.[28]

In the failing heart, ventricular myocytes showed a significant increase in SK currents compared with the normal ventricular myocytes possibly as a result of the increased sensitivity of SK channels to intracellular Ca^{2+}.[27] In a rabbit model with HF and spontaneous ventricular fibrillation, apamin eliminated the recurrent spontaneous ventricular fibrillation.[29] On the other hand, intracellular calcium cycling is a target of renin–angiotensin–aldosterone system activation to develop cardiac hypertrophy. The release of calcium is related to the ryanodine receptor (RyR2) in the heart by SR Ca^{2+}-ATPase (SERCA pump), and abnormalities of Ca^{2+} handling appear to be arrhythmogenic. The effect of RAS inhibitors on SERCA pump and loss function of K^+ currents is powerful to normalize the intracellular calcium handling and the repolarization process of K^+ currents control, possibly contributing to their anti-arrhythmic effects in this condition.[30–32] As a result, SV with synergistic effect of RAS and neprilysin inhibition improved electromechanical remodelling with diastolic dysfunction in SHR. On the other hand, cBIN-1 was overexpressed in SHR group and reduced after treatment with SV, rather than valsartan. The level of cBIN-1 is reduced in animal models of HF, as well as in human biopsy samples from patients with end-stage cardiomyopathy.[16,33,34] The present study firstly demonstrated that SV therapy up-regulated the tissue expression of cBIN-1 and the up-regulation was beneficial for ventricular arrhythmia and remodelling.

In conclusion, SV therapy led to a greater reversal of ventricular hypertrophy, improvement of diastolic function, amelioration of arrhythmic inducibility, and reduction of cardiac fibrosis, caused by down-regulation of SK2 channel and up-regulation of cBIN-1, as compared with valsartan therapy and controls. The anti-arrhythmic effects of SV could be explained not only indirectly by reducing myocardial cell death, hypertrophy, fibrosis, and inflammation but also directly by improving intracellular Ca^{2+} handling via T-tubule and SK2 channels.

Limitations

Firstly, the anaesthetic protocol could influence the electrophysiological property of the heart. Previous study has shown that isoflurane lowers HR, disrupts Doppler measurements, and can give false measurements of ventricular relaxation as well as systolic parameters.[35] Secondly, while HF in SHR occurs around 2 years of age, data regarding the presence of HF with preserved ejection in this model are limited and confusing. This inbred strain is predisposed to hypertension and

more similar to essential hypertension in humans.[36] In our study, the young SHR without obvious HF symptoms only represents the murine model of hypertensive heart disease, characterized by ventricular hypertrophy, cardiac fibrosis, and diastolic dysfunction, rather than the murine model of HF with preserved ejection.[36]

Conclusions

Hypertension is well known to contribute to the progression of LVH and diastolic dysfunction and eventually resulted in hypertensive heart disease. Targeting both of the neprilysin and angiotensin II systems would be a novel approach in the treatment of the severe hypertension-related disease. This study was the first to evaluate mechanism of anti-arrhythmic effect in SV across down-regulation of SK2 channel in SHRs. The SHR model shares many common features with hypertensive heart disease, including ventricular hypertrophy, diastolic dysfunction, and cardiac fibrosis. This study opens the door to the therapeutic potential of targeting cardiac SK2 channel by SV because it could prevent repolarization heterogeneity and interstitial fibrosis to abolish arrhythmogenesis.

Conflict of interest

None declared.

Funding

This work was supported by the Science and Technology Unit, Ministry of Health and Welfare, Executive Yuan, Taiwan (106-2314-B-002-046-MY2), Grants 105-HCH065, 106-HCH004, 106-HCH056, and 107-HCH010 from the National Taiwan University Hospital Hsin-Chu Branch, and Collaborative Research Grants 104W970 and 105W970 from the National Chiao Tung University.

References

1. Yancy CW, Jessup M, Bozkurt B, Butler J, Casey DE Jr, Drazner MH, Fonarow GC, Geraci SA, Horwich T, Januzzi JL, Johnson MR, Kasper EK, Levy WC, Masoudi FA, McBride PE, McMurray JJ, Mitchell JE, Peterson PN, Riegel B, Sam F, Stevenson LW, Tang WH, Tsai EJ, Wilkoff BL, American College of Cardiology Foundation, American Heart Association Task Force on Practice Guidelines. 2013 ACCF/AHA guideline for the management of heart failure: a report of the American College of Cardiology Foundation/American Heart Association Task Force on Practice Guidelines. *J Am Coll Cardiol* 2013; **62**: e147–e239.
2. Cho JH, Zhang R, Kilfoil PJ, Gallet R, de Couto G, Bresee C, Goldhaber JI, Marban E, Cingolani E. Delayed repolarization underlies ventricular arrhythmias in rats with heart failure and preserved ejection fraction. *Circulation* 2017; **136**: 2037–2050.
3. Vaduganathan M, Patel RB, Michel A, Shah SJ, Senni M, Gheorghiade M, Butler J. Mode of death in heart failure with preserved ejection fraction. *J Am Coll Cardiol* 2017; **69**: 556–569.
4. Owan TE, Hodge DO, Herges RM, Jacobsen SJ, Roger VL, Redfield MM. Trends in prevalence and outcome of heart failure with preserved ejection fraction. *N Engl J Med* 2006; **355**: 251–259.
5. SOLVD Investigators*. Effect of enalapril on survival in patients with reduced left ventricular ejection fractions and congestive heart failure. *N Engl J Med* 1991; **325**: 293–302.
6. Iborra-Egea O, Gálvez-Montón C, Roura S, Perea-Gil I, Prat-Vidal C, Soler-Botija C, Bayes-Genis A. Mechanisms of action of sacubitril/valsartan on cardiac remodeling: a systems biology approach. *NPJ Syst Biol Appl* 2017; **3**: 12.
7. Martens P, Nuyens D, Rivero-Ayerza M, Van Herendael H, Vercammen J, Ceyssens W, Luwel E, Dupont M, Mullens W. Sacubitril/valsartan reduces ventricular arrhythmias in parallel with left ventricular reverse remodeling in heart failure with reduced ejection fraction. *Clin Res Cardiol* 2019; **108**: 1074–1082.
8. de Diego C, Gonzalez-Torres L, Nunez JM, Centurion Inda R, Martin-Langerwerf DA, Sangio AD, Chochowski P, Casasnovas P, Blazquez JC, Almendral J. Effects of angiotensin-neprilysin inhibition compared to angiotensin inhibition on ventricular arrhythmias in reduced ejection fraction patients under continuous remote monitoring of implantable defibrillator devices. *Heart Rhythm* 2018; **15**: 395–402.
9. Chang P-C, Lin S-F, Chu Y, Wo H-T, Lee H-L, Huang Y-C, Wen M-S, Chou C-C. LCZ696 therapy reduces ventricular tachyarrhythmia inducibility in a myocardial infarction-induced heart failure rat model. *Cardiovasc Ther* 2019; **2019**: 1–9.
10. Torrado J, Cain C, Mauro AG, Ockaili RA, Romeo F, Nestler J, Devarakonda T, Das A, Salloum FN. Sacubitril/valsartan attenuates fibrosis and improves left ventricular function in a rabbit model of HFrEF. *Circulation* 2017; **136**: A24021-A24021.
11. Verdecchia P, Angeli F, Cavallini C, Aita A, Turturiello D, De Fano M, Reboldi G. Sudden cardiac death in hypertensive patients. *Hypertension* 2019; **73**: 1071–1078.
12. Tomaselli GF, Zipes DP. What causes sudden death in heart failure? *Circ Res* 2004; **95**: 754–763.
13. Monsuez JJ, Papon BJ, Lachurie ML, Passeron J. Sudden cardiac death in heart failure: the role of abnormal repolarization. *Circulation* 1995; **91**: 1899–1900.
14. Manolis AS, Manolis AA, Manolis TA, Melita H. Sudden death in heart failure with preserved ejection fraction and beyond: an elusive target. *Heart Fail Rev* 2019; **24**: 847–866.
15. Vaduganathan M, Claggett BL, Chatterjee NA, Anand IS, Sweitzer NK, Fang JC, O'Meara E, Shah SJ, Hegde SM, Desai AS, Lewis EF, Rouleau J, Pitt B, Pfeffer MA, Solomon SD. Sudden death in heart failure with preserved ejection fraction: a competing risks analysis from the TOPCAT trial. *JACC Heart Fail* 2018; **6**: 653–661.
16. Nikolova AP, Hitzeman TC, Baum R, Caldaruse AM, Agvanian S, Xie Y, Geft

DR, Chang DH, Moriguchi JD, Hage A, Azarbal B, Czer LS, Kittleson MM, Patel JK, Wu AHB, Kobashigawa JA, Hamilton M, Hong T, Shaw RM. Association of a novel diagnostic biomarker, the plasma cardiac bridging integrator 1 score, with heart failure with preserved ejection fraction and cardiovascular hospitalization. *JAMA Cardiol* 2018; **3**: 1206–1210.
17. Messerli FH, Bangalore S, Bavishi C, Rimoldi SF. Angiotensin-converting enzyme inhibitors in hypertension: to use or not to use? *J Am Coll Cardiol* 2018; **71**: 1474–1482.
18. Walker MJ, Curtis MJ, Hearse DJ, Campbell RW, Janse MJ, Yellon DM, Cobbe SM, Coker SJ, Harness JB, Harron DW, Higgins AJ. The Lambeth Conventions: guidelines for the study of arrhythmias in ischaemia infarction, and reperfusion. *Cardiovasc Res* 1988; **22**: 447–455.
19. Gu M, Zhu Y, Yin X, Zhang DM. Small-conductance Ca^{2+}-activated K^{+} channels: insights into their roles in cardiovascular disease. *Exp Mol Med* 2018; **50**: 23.
20. Chang PC, Chen PS. SK channels and ventricular arrhythmias in heart failure. *Trends Cardiovasc Med* 2015; **25**: 508–514.
21. Tamarappoo BK, John BT, Reinier K, Teodorescu C, Uy-Evanado A, Gunson K, Jui J, Chugh SS. Vulnerable myocardial interstitium in patients with isolated left ventricular hypertrophy and sudden cardiac death: a postmortem histological evaluation. *J Am Heart Assoc* 2012; **1**: e001511.
22. Mazzolai L, Pedrazzini T, Nicoud F, Gabbiani G, Brunner H-R, Nussberger J. Increased cardiac angiotensin II levels induce right and left ventricular hypertrophy in normotensive mice. *Hypertension* 2000; **35**: 985–991.
23. Hubers SA, Brown NJ. Combined angiotensin receptor antagonism and neprilysin inhibition. *Circulation* 2016; **133**: 1115–1124.
24. McMurray JJV, Jackson AM, Csp L, Redfield MM, Anand IS, Ge J, Lefkowitz MP, Maggioni AP, Martinez F, Packer M, Pfeffer MA, Pieske B, Rizkala AR, Sabarwal SV, Shah AM, Shah SJ, Shi VC, van Veldhuisen DJ, Zannad F, Zile MR, Cikes M, Goncalvesova E, Katova T, Kosztin A, Lelonek M, Sweitzer N, Vardeny O, Claggett B, Jhund PS, Solomon SD. Effects of sacubitril-valsartan versus valsartan in women compared with men with heart failure and preserved ejection fraction: insights from PARAGON-HF. *Circulation* 2020; **141**: 338–351.
25. Swissa M, Qu Z, Ohara T, Lee MH, Lin SF, Garfinkel A, Karagueuzian HS, Weiss JN, Chen PS. Action potential duration restitution and ventricular fibrillation due to rapid focal excitation. *Am J Physiol Heart Circ Physiol* 2002; **282**: H1915–H1923.
26. Nguyen TP, Sovari AA, Pezhouman A, Iyer S, Cao H, Ko CY, Bapat A, Vahdani N, Ghanim M, Fishbein MC, Karagueuzian HS. Increased susceptibility of spontaneously hypertensive rats to ventricular tachyarrhythmias in early hypertension. *J Physiol* 2016; **594**: 1689–1707.
27. Zhang XD, Lieu DK, Chiamvimonvat N. Small-conductance Ca^{2+}-activated K^{+} channels and cardiac arrhythmias. *Heart Rhythm* 2015; **12**: 1845–1851.
28. Hsieh YC, Chang PC, Hsueh CH, Lee YS, Shen C, Weiss JN, Chen Z, Ai T, Lin SF, Chen PS. Apamin-sensitive potassium current modulates action potential duration restitution and arrhythmogenesis of failing rabbit ventricles. *Circ Arrhythm Electrophysiol* 2013; **6**: 410–418.
29. Chua SK, Chang PC, Maruyama M, Turker I, Shinohara T, Shen MJ, Chen Z, Shen C, Rubart-von der Lohe M, Lopshire JC, Ogawa M, Weiss JN, Lin SF, Ai T, Chen PS. Small-conductance calcium-activated potassium channel and recurrent ventricular fibrillation in failing rabbit ventricles. *Circ Res* 2011; **108**: 971–979.
30. Flesch M, Schiffer F, Zolk O, Pinto Y, Stasch JP, Knorr A, Ettelbrück S, Böhm M. Angiotensin receptor antagonism and angiotensin converting enzyme inhibition improve diastolic dysfunction and Ca^{2+}-ATPase expression in the sarcoplasmic reticulum in hypertensive cardiomyopathy. *J Hypertens* 1997; **15**: 1001–1009.
31. Takeishi Y, Bhagwat A, Ball NA, Kirkpatrick DL, Periasamy M, Walsh RA. Effect of angiotensin-converting enzyme inhibition on protein kinase C and SR proteins in heart failure. *Am J Physiol Heart Circ Physiol* 1999; **276**: H53–H62.
32. Giudicessi JR, Ackerman MJ. Potassium-channel mutations and cardiac arrhythmias—diagnosis and therapy. *Nat Rev Cardiol* 2012; **9**: 319–332.
33. Shah SJ, Aistrup GL, Gupta DK, O'Toole MJ, Nahhas AF, Schuster D, Chirayil N, Bassi N, Ramakrishna S, Beussink L, Misener S, Kane B, Wang D, Randolph B, Ito A, Wu M, Akintilo L, Mongkolrattanothai T, Reddy M, Kumar M, Arora R, Ng J, Wasserstrom JA. Ultrastructural and cellular basis for the development of abnormal myocardial mechanics during the transition from hypertension to heart failure. *Am J Physiol Heart Circ Physiol* 2014; **306**: H88–H100.
34. Frisk M, Ruud M, Espe EK, Aronsen JM, Roe AT, Zhang L, Norseng PA, Sejersted OM, Christensen GA, Sjaastad I, Louch WE. Elevated ventricular wall stress disrupts cardiomyocyte t-tubule structure and calcium homeostasis. *Cardiovasc Res* 2016; **112**: 443–451.
35. Sarkar S, GuhaBiswas R, Rupert E. Echocardiographic evaluation and comparison of the effects of isoflurane, sevoflurane and desflurane on left ventricular relaxation indices in patients with diastolic dysfunction. *Ann Card Anaesth* 2010; **13**: 130–137.
36. Valero-Munoz M, Backman W, Sam F. Murine models of heart failure with preserved ejection fraction: a "fishing expedition". *JACC Basic Transl Sci* 2017; **2**: 770–789.